ELSEVIER

Journal of Nuclear Materials 258–263 (1998) 1842–1847

journal of nuclear materials

Damage structure evolution in Al_2O_3 irradiated with multiple ion beams of H, He and O and after annealing

Y. Katano *, T. Nakazawa, D. Yamaki, T. Aruga, K. Noda

Department of Materials Science and Engineering, Japan Atomic Energy Research Institute, Tokai, Ibaraki 319-11, Japan

Abstract

Damage structures in a single crystal Al_2O_3 sample irradiated at 923 K with simultaneous triple beams of H-, He- and O-ions with respective energies of 0.25, 0.9 and 4.7 MeV up to a fluence of 2.7, 3.5 and 5.5×10^{20} m^2, were examined by cross-section electron microscopy. High density dislocation loops are formed to a depth of 2.4 μm and the loop density increases with increasing depth. Cavities are observed in bands with the swelling peaked at depths of 1.4, 1.9 and 2.3 μm for H-, He- and O-ion implanted regions, respectively. The growth of cavities is most pronounced in the O-ion damaged region with a maximum size of 13 nm and a density of $2–3 \times 10^{23} m^3$. In a sample annealed for 1 h at 1273 K after the irradiation, cavities grown to an average size 40 and 60 nm with a maximum of 70 nm were observed in He- and O-ion implanted regions, respectively, and the density was decreased by about two orders.

1. Introduction

Alumina (Al_2O_3) has been proposed for electrical insulators and diagnostic materials in fusion reactors, because of its excellent electrical and optical properties [1,2]. In the fusion reactor environment, the generation rates of H and He in Al_2O_3 are estimated to be 170–190 appm/dpa (dpa; displacement per atom) [3]. The effects of displacement damage under the coexistence of He and/or H atoms upon the damage structure have been studied by simultaneous multiple ion beam irradiation techniques [4–8]. However, synergetic effects of atomic displacement damage with H and He atom production, under fusion reactor simulated environments, have not been clarified yet.

In the present study, we have investigated the damage structures in Al_2O_3 samples simultaneously irradiated with beams of self oxygen (O) ions, and hydrogen (H) and helium (He) gas atom ions, and after a post-irradiation anneal at a high temperature by a cross-section transmission electron microscopy (XTEM). The results are discussed in terms of the implantation rates of H and He atoms per dpa using the depth profiles of swellings measured for the as-irradiated samples.

2. Experimental procedure

The material used in this study was single crystal alumina (α-Al_2O_3). The results of chemical analysis of the materials have been reported elsewhere [9]. Disk samples of 0.2 mm in thickness and 10 mm in diameter with surface perpendicular to (0 0 0 1) planes were polished optically flat and then annealed at 1273 K for 4 h under air by a furnace, followed by cooling in the furnace with a rate of 2°C/min.

Irradiation was carried out using the "triple ion beam facility" in Takasaki Ion Accelerator facility for Advanced Radiation Application (TIARA) at Takasaki-establishment of JAERI. The sample was irradiated with simultaneous triple ion beams (0.25 MeV H^+, 0.9 MeV He^+ and 4.7 MeV O^{2+}) up to ion fluences of 2.7 to 5.5×10^{20} ion/m^2 at 923 K (0.4Tm). The ion energies were so chosen that most of O-ions stop around a distance of 2.2 μm from the incident surface after traversing the H- and He-ion implanted regions. The depth-dependent displacement damage levels (displacements per atom, dpa) associated with the ion irradiations were

* Corresponding author. Tel.: +81 29 282 5435; fax: +81 29 282 5460; e-mail: katano@maico.tokai.jaeri.go.jp.

0022-3115/98/$19.00
PII: S0022-3115(98)00410-3

Table 1
Triple beam irradiation (#95-09) conditions and corresponding damage parameters obtained by TRIM calculations

Energy/Ion (MeV)	Flux (10^{16} ions/m^{2}s)	Fluence (10^{20} ions/m^2)	Calculated value (TRIM)			
			Damage peak depth (μm)	Peak damage (dpa)	Average projected range (μm)	Peak ion concentration (at. %)
0.25 H^+	1.6	2.7	1.35	0.05	1.38	2.0
0.9 He^+	2.0	3.5	1.85	0.7	1.90	2.0
4.7 O^{2+}	3.2	5.5	2.10	7.6	2.18	3.2

determined with the TRIM89 Code [10] using a threshold displacement energy of 40 eV [3]. Table 1 summarizes the irradiation conditions and damage parameters, depth profiles of which are shown in Fig. 3(c). This irradiation with triple ion beams makes it possible for H and He atoms to be implanted with synergistic displacement damage levels as high as 1–1.5 and 4–5.5 dpa for H- and He-ion implanted regions, respectively.

After irradiation, a specimen for TEM was prepared using the cross-section method: mechanical grinding and dimpling to a thickness of about 20 μm, and ion milling with 6 keV Ar ions using a liquid nitrogen-cooled stage. TEM observation was performed for the as-irradiated sample and that annealed for 1 h at 1273 K, using a JEM-2000FX electron microscope operating at 200 kV. The foil thickness was estimated by counting the number of equal thickness fringes from the foil edge. The defect density and diameter were determined using micrographs with final magnifications of $1.1–2.2 \times 10^5$.

3. Experimental results

3.1. Microstructures after irradiation

The cross-section microstructure of Al_2O_3 irradiated with triple (H^+, He^+ and O^{2+}) beams at 923 K are shown in Fig. 1. The damaged region extends from the position very close to the ion-incident surface to a depth of 2.4 μm (Fig. 1(a) and (b)). A high density of dislocation loops is formed to a depth of 2.4 μm and the dislocation density increases with increasing depths, while the average sizes decrease from ~150 nm near the irradiation surface to smaller sizes for larger depths. The range of depths where loops are observed is comparable to the predicted end-of-range for O-ions. No distinguished features indicating separate damage regions due to implanted H- and He-ions are discernible in the dislocation structure.

Cavities are observed to be formed from 0.3 to 2.4 μm in depth, and apparently in three bands with swelling peaked at depths of 1.4, 1.9 and 2.3 μm for the H-, He- and O-ion damaged regions, respectively. These depths are comparable to the calculated damage peak depths (Table 1, Fig. 3(c)), for the respective ion. However, irregularly shaped and relatively larger sized cavities observed at depths around O-ion's range are seen distributed about 10% deeper than the O-ion's average predicted range or the damage peak, and the sizes tend to become smaller with a decrease in the depth. Cavities around the He-ion implanted region are observed to be aligned in the ⟨0 0 0 1⟩ direction. The cavity alignment is observed for a depth region from 1.6 to 2.0 μm, which agrees with the calculated region of depths for stopped He-ions (Figs. 1(b) and 3(c)). Although the growth of cavities is seemingly most pronounced in the O-ion damaged region with a maximum size of 13 nm, the cavity density is seen to be peaked at depths around the He-ion's average projected range. This is because in addition to relatively large cavities as observed with sizes of 7–12 and 5 nm in the O- and He-ion implanted regions, respectively, tiny cavities sized below 1 nm with an exceedingly high density were observed at depths from 1.5 to 2.3 μm.

The cavity densities and average sizes measured in 0.1 or 0.05 μm depth intervals are given in Fig. 3(a). The cavity density is peaked at 3.5×10^{23} m^3 around a depth of 1.9 μm. In contrast, the average size is peaked around a depth of 1.5 μm and tends to decrease with an increase in depth or damage level, at least up to 1.8 μm. This is understood by the fact that, in the cavity size distributions, more than 80% of the observed cavities are sized below 1 nm for He- and O-ion implanted region of depths: for example, one 10-nm sized cavity existing with ten 1-nm sized cavities result in an average size of less than 2 nm. Resultant swellings as obtained from these size distribution are plotted as a function of depths in Fig. 4, showing that cavity swelling in H- and He-ion implanted region are less than 0.2% for damage levels from 1 to 6 dpa. Moreover, swelling in the He-ion implanted region is observed to be depressed. Conversely, the swelling around O-ion implanted region sharply increases to 1%.

3.2. Microstructures after post-irradiation annealing

The microstructures observed in the sample annealed for 1 h at 1273 K after the triple beam irradiation are shown in Fig. 2. Note that a remarkable annealing of the dislocation loops occurs for all damaged region of

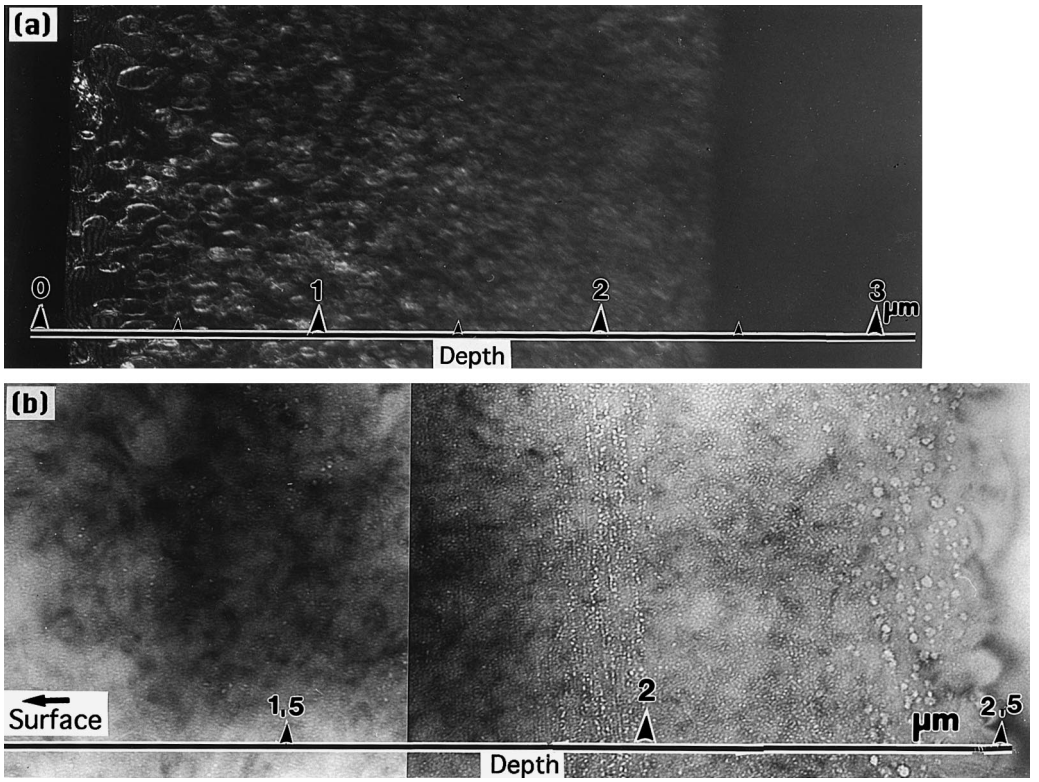

Fig. 1. Cross-section damage structures in single crystal Al_2O_3 irradiated with triple (H^+, He^+ and O^{2+}) beams at 923 K; (a) a dislocation component in dark field image and (b) a cavity component.

depths of 0–2.4 μm (Fig. 2(a)) dislocation lines, mostly grown to long segments, are distributed up to depths around 3 μm.

Cavities extraordinarily grown to 50–70 nm at the maximum size are observed for a region of depths of 1.7–2.6 μm (Fig. 2(b)), with the number density of cavities being decreased to $1–2 \times 10^{21}$ m^3, smaller by about two orders than that in the as-irradiated sample. This indicates that cavities have coalesced remarkably during the annealing, with a resultant swelling of maximum 8% for a region of depths of 2.4–2.5 μm, for example. These large cavities in these depths are observed to be slightly facetted to form a hexagonal shape. Compared with cavities grown to large sizes of 30–70 nm in an average for He- and O-ion implanted region, the cavity growth is less pronounced for depths smaller than 1.5 μm, where damage levels are lower than 1.5 dpa.

Depth profiles of cavity size and density measured in the annealed sample for the same representative regions of depths as above are given in Fig. 3(b), and resultant cavity swelling as a function of depth in Fig. 4. An appearance of a large dip in the depth profile of swelling around a depth of 1.3 μm indicates that, although cavity growth in the annealed sample is seen to be dominated by the accumulated displacement damage levels, as is evidenced by a growth of cavities observed in a much lower density in depths between the two swelling peaks (Fig. 2(b)), the growth is also strongly influenced by the presence of implanted He-atoms.

4. Discussion

The present triple ion beam irradiation renders an investigation on microstructural evolutions using one irradiated Al_2O_3 sample for both hydrogen and helium production rates nominally ranging from 0 to 2×10^4 appm-H/dpa and 0 to 5×10^3 appm-He/dpa, although damage levels are restricted to be a narrow range of 1–1.5 and 4–5.5 dpa, respectively (Fig. 3(c)). Separate influences of H and He gas atoms under simultaneous displacement damages have thus been examined.

The present cavity formation behavior around the H-ion implanted region differs from the previous observation [8]: small cavities formed inhomogeneously along dislocation loops grown to a large size with a swelling of 0.3% dpa, which is about three times larger than 0.1% dpa observed in the present sample around 1.4 μm. Besides, formation of cavities along grown loops is not so clearly observed. These features of homogeneous

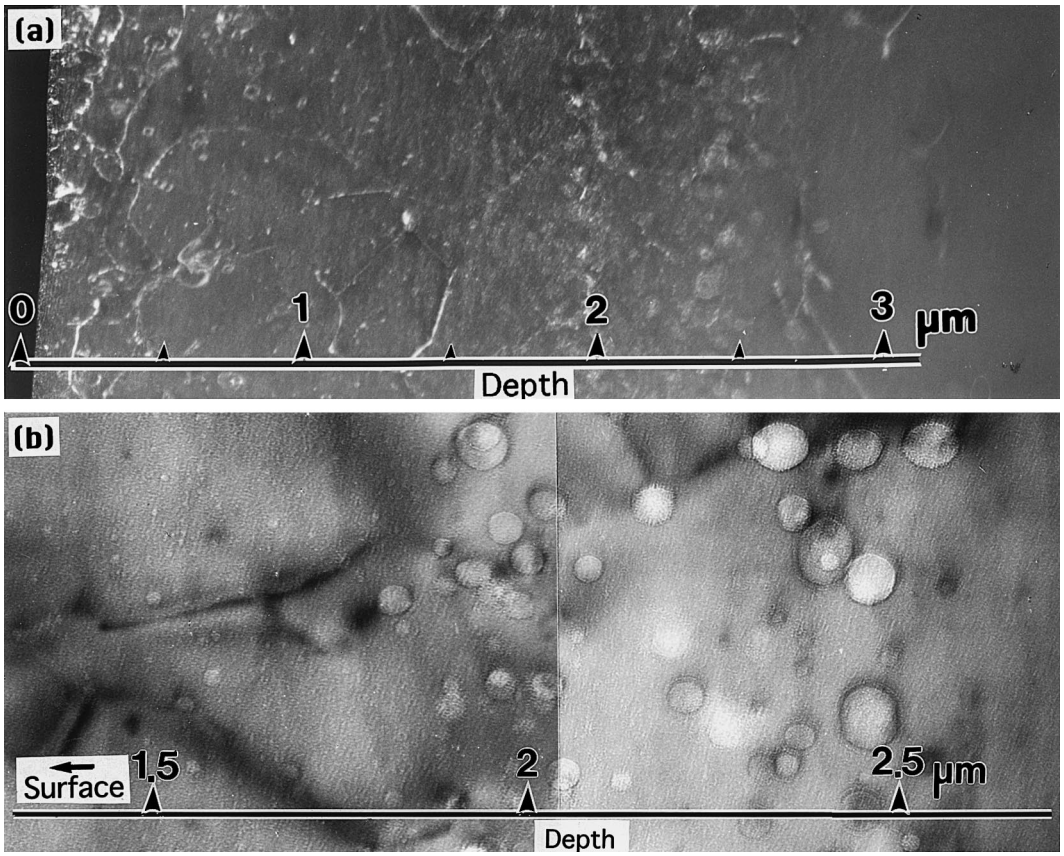

Fig. 2. Cross-section damage structure in Al_2O_3 annealed for 1 h at 1273 K after the irradiation with triple (H^+, He^+ and O^+) beams at 923 K; (a) dislocation component in a dark field image and (b) a cavity component.

cavity formation with small swelling per unit dpa suggest that an increased damage level due to O-ions traversing the H-ion implanted region may hinder H-atoms from flowing into loops and forming cavities along loops, possibly through trapping at defect clusters (dislocation loops) due to the energetic O-ion displacement cascades.

In contrast with a disappearance of cavity formation along loops in the H-ion implanted region, the formation of cavities aligned to *c*-axis, as has previously been observed in alumina samples irradiated with neutrons [11] and with simultaneous triple ion beams [5,8], is observed up to a higher damage level of 4–5.5 dpa for He-ion implanted region of depths. Swelling due to these cavities is smaller than 0.2% (Fig. 4). Around a depth of 1.9 μm (corresponding to the peak He density), it is as low as 0.01%, possibly due to an increased cavity nucleation which would suppress its growth.

Cavity swelling per unit dpa may vary with the implantation rates expressed as appm-He/dpa. Using presently measured swelling data as a function of depth along with the calculated depth profiles of damage parameters (Fig. 3(c)), swelling rates defined here as swelling per unit dpa are plotted in Fig. 5 as a function of appm-He/dpa for He atoms implanted under the concurrent damage due to O-ions. For comparison, data against appm-H/dpa are also plotted in the figure. Although data of swelling rates are scattered inevitably due to poor statistics of counting number densities of cavities and steep gradients of He and H atom distributions, a rough trend for cavity formation behavior under the present irradiation is quantitatively exhibited: namely, swelling per unit dpa decreased with increasing appm-He/dpa up to a value around several hundreds of appm-He/dpa, then changed into an increase. On the other hand, increasing appm-H/dpa values from 100 to 2×10^4 leads to a very rapid decrease in swelling rates.

The increased growth of cavities observed in the sample annealed at 1273 K for 1 h after the irradiation signifies that alumina, if it is subjected under a high temperature around 1273 K after an irradiation to 4–8 dpa at a lower temperature, may swell as much as 8% in the volumic fraction. The observed strain fields for cavities in the region of depths suggest that cavities are

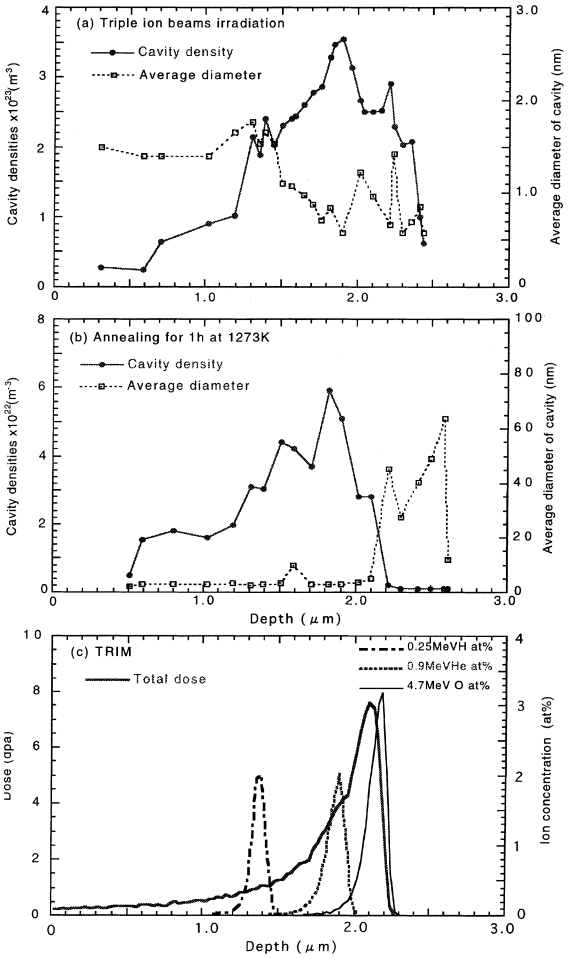

Fig. 3. Depth profiles of cavity formation behavior measured in the Al_2O_3 irradiated with triple beams at 923 K (a) and in the sample subsequently annealed for 1 h at 1273 K (b) and depth profiles of damage parameters for the triple beam irradiation obtained by TRIM89 (c).

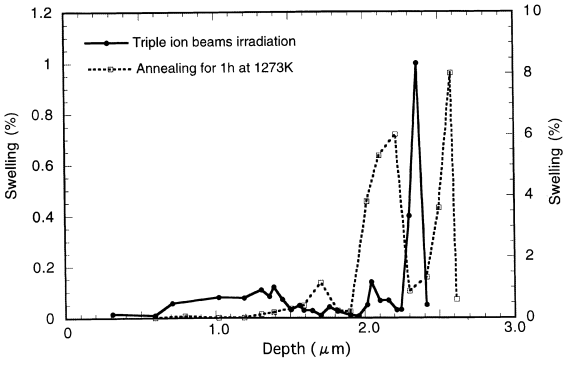

Fig. 4. Depth profiles of swelling in the Al_2O_3 irradiated with triple beams at 923 K and in the sample subsequently annealed for 1 h at 1273 K.

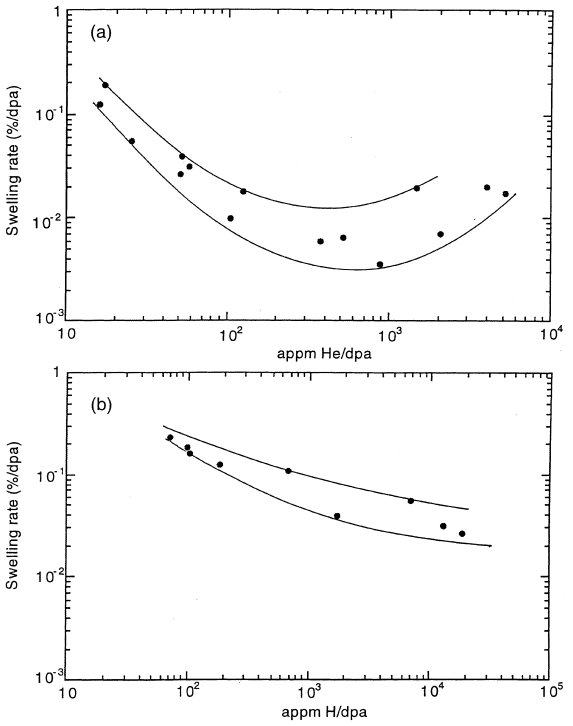

Fig. 5. Swelling per unit dpa as a function of He– (a) and H– (b) atom implantation rate in the Al_2O_3 irradiated with triple beams at 923 K. Lines are drawn as a guide for the eye.

bubbles over-pressurized due to implanted He and O atoms. On the other hand, H atoms implanted to the same concentration as He atoms, however, contribute much less to cavity growth, probably through escaping from the lattice by a much faster, pipe diffusion along climbing dislocations during annealing.

5. Summary

The microstructural evolution in single crystal α-Al_2O_3 due to the irradiation at 923 K with triple beams of H^+, He^+ and O^{2+} ions, and in the sample annealed at 1273 K for 1 h after the irradiation, has been studied by XTEM, and main results summarized are as follows:

1. Cavities were formed from 0.3 to 2.4 μm in depth, and apparently in three bands with swellings peaked at depths of 1.4, 1.9 and 2.3 μm for H-, He- and O-ion implanted regions, respectively.
2. Swelling per unit dpa was seen to have a minimum for appm-He/dpa ratios of about several hundred for doses of about 1–5 dpa.
3. Increased growth of cavities occurred after annealing for 1 h at 1273 K for He- and O-ion implanted region of depths, which resulted in a swelling of 7–8%.

Acknowledgements

The authors wish to express their thanks to the staff in the accelerator facility of Takasaki establishment of JAERI for their invaluable help, and to Drs. H. Katsuta and H. Nakajima for support and encouragement.

References

[1] F.W. Clinard Jr., J. Nucl. Mater. 85&86 (1979) 393.
[2] G.R. Hopkins, R.J. Price, Nucl. Eng. Des. Fusion 2 (1985) 111.
[3] G.P. Pells, J. Nucl. Mater. 155–157 (1988) 67.
[4] W.E. Lee, M.L. Jenkins, G.P. Pells, Philos. Mag. A51 (1985) 639.
[5] S.J. Zinkle, S. Kojima, J. Nucl. Mater. 179–181 (1991) 395.
[6] S.J. Zinkle, Nucl. Instr. and Meth. B 91 (1994) 234.
[7] S.J. Zinkle, J. Nucl. Mater. 219 (1995) 113.
[8] Y. Katano, T. Nakazawa, D. Yamaki, T. Aruga, K. Noda, J. Nucl. Mater. 233–237 (1996) 1325.
[9] Y. Katano, H. Ohno, H. Katsuta, J. Nucl. Mater. 155–157 (1988) 366.
[10] J.F. Ziegler, J.P. Biersak, U.L. Littmark, The Stopping and Range of Ions in Solids, Pergamon, New York, 1985.
[11] F.W. Chinard Jr., G.F. Hurley, L.W. Hobbs, J. Nucl. Mater. 108&109 (1982) 655.